Pose Observers for Unmanned Air Vehicles

S. Brás

***Abstract*—This paper addresses the design and discrete time implementation of nonlinear observers for the estimation of position and attitude in 3D with application to Unmanned Air Vehicles. A continuous time nonlinear observer on SE(3) is derived that uses inertial measurements and ranges between a set of beacons mounted in a fixed location in an inertial frame and a receiver array installed on the vehicle frame. The estimation errors are shown to converge exponentially fast to the desired equilibrium points in the presence of bias in the rate gyros. An observer discrete time implementation is proposed that resorts to recent geometric numeric integration results suitable for solving ODEs on SO(3). Simulation results for oscillatory trajectories of the vehicle are presented to assess the performance of the continuous time observer versus that obtained with the discrete time implementation.**

I. INTRODUCTION

Attitude and position estimation is a classical problem often subject to new advances and enriching insights, despite its wide historical background. Among a large diversity of estimation techniques, nonlinear observers stand out as a promising approach often endowed with stability results.

Research on the problem of deriving a stabilizing law for systems evolving on manifolds, namely SO(3) and SE(3), can be found in [5], [7], [12], [15], [22], that provide important guidelines for observer design, due to the realized discussion on the topological characteristics and limitations for achieving global stabilization on the SO(3) manifold.

In many applications it is desired to design observers based only on the rigid body kinematics. These observers have the advantage of that kinematics is an exact description of the physical quantities involved, requiring however, a larger number of sensors [25], [26], [27], [1]. In [14], an asymptotically stable attitude observer on SO(3) is derived using attitude and biased angular velocity readings. The nonlinear attitude observer proposed in [24], is formulated using the quaternion representation, to obtain global exponentially convergence to the origin given attitude measurements and biased inertial readings. In these references the observer is assuming that a perfect attitude information, rotation matrix or quaternion, is available, obtained by pre-processing information such as image based features, landmark measurements, and vector readings. However, this is not considered in the observer design and it can compromise its stability.

The development of numeric integration methods that preserve geometric properties, has witnessed in last fifteen years a remarkable progress, and particular emphasis was placed by the scientific community on integration methods for integration of differential equations evolving on a Lie group. These methods were originally proposed by Crouch and Grossman in [6], and the general order conditions computed in [20]. In [17] the author construct generalized Runge-Kutta methods for integration of differential equations evolving on Lie groups, where the computations are performed in the Lie algebra, which is a linear space. More recently, in [4, 19], authors derive the order conditions for commutator free Lie group methods, to overcome some of the problems associated with the computation of commutators.

In this work, an attitude and position nonlinear observer is proposed. The observer integrates measurements from inertial sensors, accelerometers and rate gyros, with ranges provided by an acoustic positioning system. The latter is composed by an ultrasonic beacon array assumed fixed in the inertial frame and an acoustic receiver array installed on the vehicle. The range data supplied by the acoustic positioning system is processed resorting to a standard spherical interpolation technique that provides the positions of the beacons in vehicle frame, and the position of the receivers in the inertial frame. By exploiting sensor information, a stabilizing feedback law is proposed and the exponential convergence to the origin of the estimation errors is shown. Using recent results from numerical analysis, an observer discrete time implementation is proposed, and its performance illustrated in simulation.

The paper is structured as follows. In Section II, the attitude and position estimation problem is introduced. The sensors considered to equip the vehicle are described and some geometric relation are introduced. In section III the attitude and position observers are proposed, and their properties are highlighted. In Section IV some recent algorithms for numeric integration in SO(3) are described. A low complexity discrete time implementation of the observer is presented in Section V, and in Section VI simulations illustrate and compare the performance of the observer and its discrete time approximation. Concluding remarks and future work are presented in Section VII.

NOMENCLATURE

The used notation is rather standard. The set of real $n \times m$ matrices is denoted as $\mathrm{M}(n,m)$ and $\mathrm{M}(n) := \mathrm{M}(n,n)$. The set of skew-symmetric, orthogonal, and special orthonormal matrices are respectively denoted as $\mathrm{K}(n) := \left\{\mathbf{K} \in \mathrm{M}(n) : \mathbf{K} = -\mathbf{K}^T\right\}$, $\mathrm{O}(n) := \left\{\mathbf{U} \in \mathrm{M}(n) : \mathbf{U}^T\mathbf{U} = \mathbf{I}\right\}$, $\mathrm{SO}(n) := \{\mathbf{R} \in \mathrm{O}(n) : \det \mathbf{R} = 1\}$. The n-dimensional sphere and ball are described by $\mathrm{S}(n) := \left\{\mathbf{x} \in \mathbb{R}^{n+1} : \mathbf{x}^T\mathbf{x} = 1\right\}$ and $\mathrm{B}(n) := \left\{\mathbf{x} \in \mathbb{R}^{n+1} : \mathbf{x}^T\mathbf{x} \leq 1\right\}$, respectively. The time dependence of variables will be omitted in general, but explicitly denoted where consider necessary.

II. PROBLEM FORMULATION

This section, introduces the sensor suite used in the attitude and position observer. The rigid body kinematics are

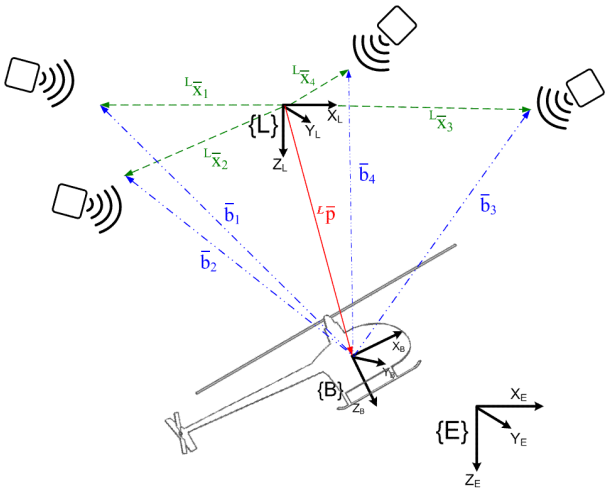

Fig. 1. Frames and navigation system configuration.

described by

$$\dot{\bar{\mathcal{R}}} = \bar{\mathcal{R}}(\bar{\boldsymbol{\omega}})^{\wedge},$$
$$\dot{\bar{\mathbf{p}}} = \bar{\mathbf{v}} - (\bar{\boldsymbol{\omega}})^{\wedge}\bar{\mathbf{p}},$$
$$\dot{\bar{\mathbf{v}}} = \bar{\mathbf{a}} + \bar{\mathcal{R}}^{T\,L}\bar{\mathbf{g}} - (\bar{\boldsymbol{\omega}})^{\wedge}\bar{\mathbf{v}},$$

where $\bar{\mathcal{R}}$ is the shorthand notation for the rotation matrix from body frame {B} to the local inertial frame {L}, $\bar{\boldsymbol{\omega}}$ is the rigid body angular velocity expressed in {B}, $\bar{\mathbf{p}}$, and $\bar{\mathbf{v}}$ are the position and velocity of the rigid body with respect to local {L} expressed in {B}, respectively, ${}^{L}\bar{\mathbf{g}}$ is the gravitational acceleration expressed in {L}, $\bar{\mathbf{a}}$ is the specific force applied to the vehicle expressed in {B}, and $(\mathbf{x})^{\wedge}$ is the skew symmetric matrix defined by the vector $\mathbf{x} \in \mathbb{R}^3$ such that $(\mathbf{x})^{\wedge}\mathbf{y} = \mathbf{x} \times \mathbf{y}$, $\mathbf{y} \in \mathbb{R}^3$.

The rigid body angular velocity is measured by a rate gyro sensor triad, corrupted by a constant bias term

$$\boldsymbol{\omega}_{sensor} = \bar{\boldsymbol{\omega}} + \bar{\mathbf{b}}_{\omega},$$

and a triaxial accelerometer measures the specific force, which is the difference between the vehicle acceleration ${}^{B}\mathbf{a}$ and the gravitational acceleration ${}^{B}\bar{\mathbf{g}}$, both in expressed in body frame,

$$\bar{\mathbf{a}} := \mathbf{a}_{sensor} = {}^{B}\mathbf{a} - {}^{B}\bar{\mathbf{g}}.$$

The acoustic positioning system gives the range from each of the beacons to the acoustic receivers installed on the vehicle. Using a spherical interpolation method [23], is possible to obtain the position of the receivers in local frame {L}, or the position of the beacons in the body frame {B}, $\bar{\mathbf{b}}_i$. In this work the latter is adopted, and the position of one of the receivers that is set as the origin of {B}, represented as ${}^{L}\bar{\mathbf{p}}$ in coordinate frame {L}. These vectors satisfy the relationship,

$$\bar{\mathbf{b}}_i = \bar{\mathcal{R}}^{T\,L}\bar{\mathbf{x}}_i - \bar{\mathcal{R}}^{T\,L}\bar{\mathbf{p}}, \tag{1}$$

where $i = 1, ..., n$, n is the number of beacons, and ${}^{L}\bar{\mathbf{x}}_i$ is the position of the *i-th* beacon in {L}. The relationship (1) can be expressed in matrix from as $\bar{\mathbf{B}} = \bar{\mathcal{R}}^{T}\mathbf{X} - \bar{\mathcal{R}}^{T\,L}\bar{\mathbf{p}}\mathbf{1}_n^{T}$, where $\bar{\mathbf{B}} := \begin{bmatrix}\bar{\mathbf{b}}_1 & ... & \bar{\mathbf{b}}_n\end{bmatrix}$, $\mathbf{X} := \begin{bmatrix}{}^{L}\bar{\mathbf{x}}_1 & ... & {}^{L}\bar{\mathbf{x}}_n\end{bmatrix}$, $\bar{\mathbf{B}}, \mathbf{X} \in \mathrm{M}(3, n)$ and $\mathbf{1}_n := [1 \ ... \ 1]^{T}$.

The local frame is defined as an inertial frame installed in the centroid of beacons. Therefore, the vectors ${}^{L}\bar{\mathbf{x}}_i$, $i = 1, ..., n$, illustrated in Fig. 1, verify

$$\sum_{i=1}^{n} {}^{L}\bar{\mathbf{x}}_i = 0.$$

The objective of the present work is to exploit the information provided by the sensor suite, by deriving a position and attitude observer that combines the inertial measurements with ranges between a beacon array and a receiver array.

III. OBSERVER SYNTHESIS

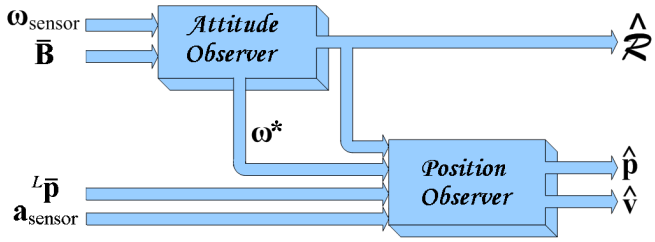

Fig. 2. Cascaded observer, composed by the attitude and the position observers.

The proposed observer is designed to match the rigid body dynamics and, as illustrated in Fig. 2, it results in a cascaded composition, where the attitude and angular velocity estimates, from the attitude observer, are fed into the position observer. In this section the attitude and position observers are presented and their properties derived. It is shown that the attitude and angular velocity bias errors converge exponentially fast to the origin and that the position observer is globally exponentially stable.

A. Attitude Observer

The attitude observer considered in this section estimates the rotation matrix by exploiting angular velocity measurements available from rate gyros, and angular position data obtained from the receiver array installed in the vehicle. Based on previews work see [25], [26], and references therein, the proposed observer estimates the orientation of the rigid body by computing the kinematics

$$\dot{\hat{\mathcal{R}}} = \hat{\mathcal{R}}(\hat{\boldsymbol{\omega}})^{\wedge}, \tag{2}$$

where $\hat{\mathcal{R}}$ is the estimated attitude, and $\hat{\boldsymbol{\omega}}$ is the feedback term that compensates for the estimation errors. Whereas the angular velocity measurements, $\boldsymbol{\omega}_{sensor}$ are used directly in the observer term $\hat{\boldsymbol{\omega}}$, the beacons positions in frame {B}, $\bar{\mathbf{b}}_i$, are introduced by means of a convenient linear coordinate transformation.

The attitude error is defined as $\tilde{\mathcal{R}} := \hat{\mathcal{R}}\bar{\mathcal{R}}^{T}$ and its dynamics are given by $\dot{\tilde{\mathcal{R}}} = \tilde{\mathcal{R}}(\bar{\mathcal{R}}(\hat{\boldsymbol{\omega}} - \bar{\boldsymbol{\omega}}))^{\wedge}$. The error matrix $\tilde{\mathcal{R}}$ can be parameterized in Euler angle-axis by a rotation vector $\boldsymbol{\lambda} \in \mathrm{S}(2)$ and by a rotation angle $\theta \in [0 \ \pi]$, yielding the formulation [18] $\tilde{\mathcal{R}} = \mathrm{rot}(\theta, \boldsymbol{\lambda}) := \cos(\theta)\mathbf{I} + \sin(\theta)(\boldsymbol{\lambda})^{\wedge} + (1 - \cos(\theta))\boldsymbol{\lambda}\boldsymbol{\lambda}^{T}$.

Consider the transformation of the positions of the beacons defined as

$$^{B}\bar{\mathbf{u}}_j := \sum_{i=1}^{n-1} a_{ij}\left(\bar{\mathbf{b}}_{i+1} - \bar{\mathbf{b}}_i\right),\ \ j = 1, ..., n-1.$$

This linear combination can be expressed in matrix form as $^{B}\bar{\mathbf{U}} := \bar{\mathbf{B}}\mathbf{D}_X\mathbf{A}_X$, where $\mathbf{D}_X := \begin{bmatrix}\mathbf{0}_{1\times n-1}\\ \mathbf{I}_{n-1}\end{bmatrix} - \begin{bmatrix}\mathbf{I}_{n-1}\\ \mathbf{0}_{1\times n-1}\end{bmatrix}$ and $\mathbf{A}_X := [a_{ij}]$. The representation of the transformation in frame $\{L\}$, is given by $\mathbf{U}_X := \bar{\mathcal{R}}\ ^{B}\bar{\mathbf{U}}_X = \begin{bmatrix}^{L}\bar{\mathbf{u}}_1 & ... & ^{L}\bar{\mathbf{u}}_{n-1}\end{bmatrix}$, and the representation using the estimate transformation is defined as $^{B}\hat{\mathbf{U}} := \hat{\mathcal{R}}\ \mathbf{U}_X = \begin{bmatrix}^{B}\hat{\mathbf{u}}_1 & ... & ^{B}\hat{\mathbf{u}}_{n-1}\end{bmatrix}$.

Proposition 1. *If* $\mathbf{H} := \mathbf{X}\mathbf{D}_X$ *has full rank, there is a non singular matrix* $\mathbf{A}_X \in \mathrm{M}(n)$*, such as,* $\mathbf{U}_X\mathbf{U}_X^T = \mathbf{I}$.

Proof: Take the SVD decomposition of $\mathbf{H} = \mathbf{U}\mathbf{S}\mathbf{V}^T$ where $\mathbf{U} \in \mathrm{O}(3)$, $\mathbf{V} \in \mathrm{O}(3)$, $\mathbf{S} = [\mathrm{diag}(s_1, s_2, s_3)\ \mathbf{0}_{3\times(n-3)}] \in \mathrm{M}(3, n)$, and $s_1 > s_2 > s_3 > 0$ are the singular values of $\mathbf{H}$. Any $\mathbf{A}_X$ given by $\mathbf{A}_X = \mathbf{V}_A\,\mathrm{blkdiag}(s_1^{-1}, s_2^{-1}, s_3^{-1}, \mathbf{B})\mathbf{V}_A^T$, where $\mathbf{B} \in \mathrm{M}(n-3)$ is non singular and $\mathbf{V}_A \in \mathrm{O}(n)$, produces $\mathbf{U}_X\mathbf{U}_X^T = \mathbf{H}\mathbf{A}_X\mathbf{A}_X^T\mathbf{H} = \mathbf{U}\mathbf{V}_A^T\mathbf{V}_A\mathbf{U}^T = \mathbf{I}$. ■

1) Unbiased Angular Velocity Measurement: Let $\bar{\mathbf{b}}_\omega = \mathbf{0}$, and consider the candidate Lyapunov function

$$\begin{aligned} V_{\mathcal{R}} &= \frac{1}{2}\sum_{i=1}^{n-1} \|^{B}\hat{\mathbf{u}}_i - {}^{B}\bar{\mathbf{u}}_i\|^2 = \mathrm{tr}\left[(\mathbf{I} - \tilde{\mathcal{R}})\mathbf{U}_X\mathbf{U}_X^T\right] = \\ &\frac{1}{4}\|\mathbf{I} - \tilde{\mathcal{R}}\|^2\boldsymbol{\lambda}^T\mathbf{P}\boldsymbol{\lambda} = (1 - \cos(\theta))\boldsymbol{\lambda}^T\mathbf{P}\boldsymbol{\lambda}, \end{aligned} \tag{3}$$

where $\mathbf{P} := \mathrm{tr}(\mathbf{U}_X\mathbf{U}_X^T)\mathbf{I} - \mathbf{U}_X\mathbf{U}_X^T \in \mathrm{M}(3)$. Choosing $\mathbf{A}_X$, such that, $\mathbf{U}_X\mathbf{U}_X^T = \mathbf{I}$, the candidate Lyapunov function (3) takes the form

$$V_{\mathcal{R}} = \mathrm{tr}\left[(\mathbf{I} - \tilde{\mathcal{R}})\right] = \frac{1}{2}\|\mathbf{I} - \tilde{\mathcal{R}}\|^2 = 2(1 - \cos(\theta)). \tag{4}$$

The Lyapunov function $V_{\mathcal{R}}$ measures the error between transformed and the actual position of the beacons, that is given by $\left\|^{B}\hat{\mathbf{u}}_i - {}^{B}\bar{\mathbf{u}}_i\right\|$, $i = 1, ..., n-1$. The estimated position of the beacons under which zero observation error is obtained ($V_{\mathcal{R}} = 0$) corresponds to the correct attitude estimate, $\tilde{\mathcal{R}} = \mathbf{I}$, and is stated in the following lemma. For the proof of Lemma 1, the reader is referred to [26].

Assumption 1. *The positions of the beacons are not colinear, i.e.* $\mathrm{rank}(\mathbf{X}) \geq 2$.

Lemma 1. *The Lyapunov function* $V_{\mathcal{R}}$ *has a unique global minimum (at* $\tilde{\mathcal{R}} = \mathbf{I}$*) if and only if Assumption 1 is verified.*

If $\mathrm{rank}(\mathbf{X}) = 2$ the conditions of Proposition 1 are not satisfied by the Assumption 1. However, in Appendix A it is shown how one can still obtain a full rank matrix by generating the direction orthogonal to the columns of $\mathbf{X}$.

The derivative of the candidate Lyapunov function (4) is

$$\dot{V}_{\mathcal{R}} = \mathbf{s}_\omega^T\left(\hat{\boldsymbol{\omega}} - \bar{\boldsymbol{\omega}}\right), \tag{5}$$

where $\mathbf{s}_\omega := \bar{\mathcal{R}}^T(\tilde{\mathcal{R}} - \tilde{\mathcal{R}}^T)^\vee = 2\sin(\theta)\bar{\mathcal{R}}^T\boldsymbol{\lambda}$ and $(.)^\vee$ is the *unskew* operator, such that, $\left((\mathbf{a})^\wedge\right)^\vee = \mathbf{a}$, $\mathbf{a} \in \mathbb{R}^3$.

In order to $V_{\mathcal{R}}$ be a Lyapunov function, a convenient attitude feedback law is defined

$$\hat{\boldsymbol{\omega}} = \bar{\boldsymbol{\omega}} - K_\omega\mathbf{s}_\omega, K_{\boldsymbol{\omega}} \in \mathbb{R}^+. \tag{6}$$

The feedback law (6), yields the autonomous attitude error system

$$\dot{\tilde{\mathcal{R}}} = K_\omega\tilde{\mathcal{R}}(\tilde{\mathcal{R}}^T - \tilde{\mathcal{R}}). \tag{7}$$

The derivative of Lyapunov function (5) together with the feedback law (6) results in

$$\dot{V}_{\mathcal{R}} = -K_\omega\|\mathbf{s}_\omega\|^2 = -K_\omega 4\sin^2(\theta), \tag{8}$$

which is negative semi-definite, so one can infer that the Lyapunov function decreases along the system trajectories. The Lyapunov function invariant set is given by

$$I_{\mathcal{R}} = \{\tilde{\mathcal{R}} \in \mathrm{SO}(3) : \tilde{\mathcal{R}} = \mathbf{I} \vee \tilde{\mathcal{R}} = \mathrm{rot}(\pi, \boldsymbol{\lambda}), \boldsymbol{\lambda} \in \mathrm{S}(2)\},$$

so for any initial condition with $\theta = \pi$, the system will not converge to the desired state $\theta = 0$. However $\theta = \pi$ is a zero measure set and, as shown in next theorem, for every other initial conditions the attitude error converges exponentially fast to the origin. The proof of this theorem is presented in [26] and references therein.

Theorem 1. *The close loop system* (7) *has a exponentially stable point at* $\tilde{\mathcal{R}} = \mathbf{I}$*, for any initial condition* $\tilde{\mathcal{R}}(t_0)$ *in the attraction region* $R_A = \{\tilde{\mathcal{R}} \in \mathrm{SO}(3) : \tilde{\mathcal{R}} = \mathrm{rot}(\theta, \boldsymbol{\lambda}), |\theta| < \pi, \boldsymbol{\lambda} \in \mathrm{S}(2)\}$*, and the trajectory satisfy*

$$\|\tilde{\mathcal{R}}(t) - \mathbf{I}\| \ \leq\ k_{\mathcal{R}}\|\tilde{\mathcal{R}}(t_0) - \mathbf{I}\|e^{-\gamma_{\mathcal{R}}(t-t_0)}, \tag{9}$$

where $k_{\mathcal{R}} = 1$ *and* $\gamma_{\mathcal{R}} = K_\omega(1 + \cos(\theta(t_0)))$

2) Biased Angular Velocity Measurement: The existence of bias in the measures of the rate gyros implies that

$$\boldsymbol{\omega}_{sensor} = \bar{\boldsymbol{\omega}} + \bar{\mathbf{b}}_\omega,$$

where bias is consider to be constant, i.e. $\dot{\bar{\mathbf{b}}}_\omega = \mathbf{0}$.

The Lyapunov function is augmented to consider the existence of bias

$$V_b = 2(1 - \cos(\theta)) + \frac{1}{2K_{b_\omega}}\|\tilde{\mathbf{b}}_\omega\|^2,$$

where $K_{b_\omega} \in \mathbb{R}^+$, $\tilde{\mathbf{b}}_\omega := \hat{\mathbf{b}}_\omega - \bar{\mathbf{b}}_\omega$, and $\hat{\mathbf{b}}_\omega$ is the estimated bias in angular velocity measurements. Its derivative is given by

$$\dot{V}_b = \mathbf{s}_\omega^T(\hat{\boldsymbol{\omega}} - \bar{\boldsymbol{\omega}}) + \frac{1}{K_{b_\omega}}\dot{\tilde{\mathbf{b}}}_\omega^T\tilde{\mathbf{b}}_\omega. \tag{10}$$

The augmented attitude feedback law is

$$\hat{\boldsymbol{\omega}} = \boldsymbol{\omega}_{sensor} - \hat{\mathbf{b}}_\omega - K_\omega\mathbf{s}_\omega = \bar{\boldsymbol{\omega}} - \tilde{\mathbf{b}}_\omega - K_\omega\mathbf{s}_\omega, \tag{11}$$

where $K_\omega \in \mathbb{R}^+$. Applying the feedback law (11) to the Lyapunov function (10) and defining

$$\dot{\tilde{\mathbf{b}}}_\omega = \dot{\hat{\mathbf{b}}}_\omega := K_{b_\omega}\mathbf{s}_\omega, \tag{12}$$

the Lyapunov function derivative is given by $\dot{V}_b = -K_\omega\|\mathbf{s}_\omega\|^2$.

Considering the feedback law (11) and the differential equation (12), the closed loop attitude error dynamics results in

$$\begin{aligned} \dot{\tilde{\mathcal{R}}} &= -K_\omega\tilde{\mathcal{R}}(\tilde{\mathcal{R}} - \tilde{\mathcal{R}}^T) - \tilde{\mathcal{R}}(\bar{\mathcal{R}}\tilde{\mathbf{b}}_\omega)^\wedge \\ \dot{\tilde{\mathbf{b}}}_\omega &= K_{b_\omega}\bar{\mathcal{R}}(\tilde{\mathcal{R}} - \tilde{\mathcal{R}}^T)^\vee \end{aligned} \tag{13}$$

Global asymptotic stability of the origin is precluded by topological limitations associated with the estimation error

$\tilde{\mathcal{R}} = \text{rot}(\pi, \tilde{\boldsymbol{\lambda}})$ [2]. In the next lemma the boundedness of estimation errors is shown and used to provide sufficient conditions that exclude convergence to the equilibrium points satisfying $\tilde{\mathcal{R}} = \text{rot}(\pi, \tilde{\boldsymbol{\lambda}})$.

Lemma 2. *The estimation errors $\tilde{\mathbf{x}}_b = (\tilde{\mathcal{R}}, \tilde{\mathbf{b}}_\omega)$ are bounded to any initial condition that verifies*

$$\frac{\frac{1}{K_{b_\omega}}\|\tilde{\mathbf{b}}_\omega(t_0)\|^2}{4(1+\cos(\theta(t_0)))} < 1 \tag{14}$$

Proof: Let $\Omega_\rho = \{\tilde{\mathbf{x}}_b \in D_b : V_b \leq \rho\}$. As the Lyapunov function (4) is a weighted distance from the origin, $\exists_\gamma \|\tilde{\mathbf{x}}_b\|^2 \leq \gamma V_b$ and Ω_ρ is a compact set. $\dot{V}_b \leq 0$ implies that any trajectory that starts in Ω_ρ remains in Ω_ρ. So, $\forall_{t\geq t_0}\|\tilde{\mathbf{x}}_b(t)\|^2 \leq \gamma V_b(\tilde{\mathbf{x}}_b(t_0))$ and the state is bounded.

The gain condition (14) is equivalent to $V_b(\tilde{\mathbf{x}}_b(t_0)) < 4$. The invariance of Ω_ρ implies that $V_b(\tilde{\mathbf{x}}_b(t)) \leq V_b(\tilde{\mathbf{x}}_b(t_0))$, and so $2(1+\cos(\theta)) \leq V_b(\tilde{\mathbf{x}}_b(t_0)) < 4$ and consequently $\exists_{\theta_{max}} : \theta(t) \leq \theta(t_0) < \theta_{max} \forall_{t\geq t_0}$. ■

Exploiting the results derived for LTV systems in [13], Theorem 2 establishes the exponential convergence of the system (13) states to the desired equilibrium point.

Theorem 2. *Assuming $\bar{\boldsymbol{\omega}}$ bounded and to any initial condition that satisfies the gain condition* (14)*, the attitude error and the bias estimation error converge exponentially fast to the equilibrium point $(\tilde{\mathcal{R}}, \tilde{\mathbf{b}}_\omega) = (\mathbf{I}, 0)$.*

Proof: Using the analysis tool for LVT parameterized systems [13], the system (13) in the form $\dot{\mathbf{x}}_b = f(t, \mathbf{x}_b)\mathbf{x}_b$ can be rewritten as $\dot{\mathbf{x}}_\star = A(\lambda, t)\mathbf{x}_\star$. The parameter λ is related with the initial conditions of the system (13). The solutions of the systems $\dot{\mathbf{x}}_b = f(t, \mathbf{x}_b)\mathbf{x}_b$ and $\dot{\mathbf{x}}_\star = A(\lambda, t)\mathbf{x}_\star$ are identic if the initial state is the same, i.e. $\mathbf{x}_\star(t_0) = \mathbf{x}_b(t_0)$.

It will be used a coordinate transformation like the one proposed in [24]. Let the attitude error be given by $\tilde{\mathbf{q}}_q = \sin\left(\frac{\theta}{2}\right)\lambda$, so the close loop dynamic is

$$\begin{aligned} \dot{\tilde{\mathbf{q}}}_q &= \frac{1}{2}\mathbf{Q}(\tilde{\mathbf{q}})(-\bar{\mathcal{R}}\tilde{\mathbf{b}}_\omega - 4K_\omega\tilde{\mathbf{q}}_q\tilde{q}_s) \\ \dot{\tilde{\mathbf{b}}}_\omega &= 4K_{b_\omega}\bar{\mathcal{R}}^T\mathbf{Q}^T(\tilde{\mathbf{q}})\tilde{\mathbf{q}}_q, \end{aligned} \tag{15}$$

where $\mathbf{Q}(\tilde{\mathbf{q}}) := \tilde{q}_s\mathbf{I} + (\tilde{\mathbf{q}}_q)^\wedge$, $\tilde{\mathbf{q}} = [\tilde{\mathbf{q}}_q^T \ \tilde{q}_s]^T$, $\tilde{q}_s = \cos\left(\frac{\theta}{2}\right)$, and $\dot{\tilde{q}}_s = -2K_\omega\tilde{\mathbf{q}}_q^T\tilde{\mathbf{q}}_q\tilde{q}_s - \frac{1}{2}\tilde{\mathbf{q}}_q^T\tilde{\mathbf{b}}_\omega$.

Let $\mathbf{x}_q := (\tilde{\mathbf{q}}_q, \tilde{\mathbf{b}}_\omega)$, $\mathbf{x}_q \in D_q$ and $D_q := \text{B}(3)\times\mathbb{R}^3$, and define the system (15) in domain $\mathcal{D}_q = \{\mathbf{x}_q \in D_q : V_b < 4\}$. The set $\mathcal{D}_q$ corresponds to the interior of the Lyapunov surface, so is well defined, and is positively invariant. The condition (14) implies that the initial state is contained in $\mathcal{D}_q$.

Let $\mathbf{x}_\star := (\tilde{\mathbf{q}}_{q\star}, \tilde{\mathbf{b}}_{\omega\star})$ and $D_q := \mathbb{R}^3 \times \mathbb{R}^3$, and define the linear time-varying system

$$\dot{\mathbf{x}}_\star = \begin{bmatrix} \mathcal{A}(t,\lambda) & \mathcal{B}^T(t,\lambda) \\ -C(t,\lambda) & \mathbf{0}_{3\times3} \end{bmatrix}\mathbf{x}_\star, \tag{16}$$

where $\lambda \in \mathbb{R}_0^+ \times \mathcal{D}_q$, and the submatrices are described by

$$\begin{aligned} \mathcal{A}(t,\lambda) &= \left[-2K_\omega\tilde{q}_s(t,\lambda)\mathbf{Q}(\tilde{\mathbf{q}}(t,\lambda))\right], \\ \mathcal{B}(t,\lambda) &= \left[-\frac{1}{2}\bar{\mathcal{R}}^T\mathbf{Q}^T(\tilde{\mathbf{q}}(t,\lambda))\right], \\ C(t,\lambda) &= \left[-4\bar{\mathcal{R}}^T\mathbf{Q}^T(\tilde{\mathbf{q}}(t,\lambda))\right], \end{aligned}$$

and $\tilde{\mathbf{q}}(t,\lambda)$ represents the solution of (15) with initial condition $\lambda = (t_0, \tilde{\mathbf{q}}(t_0), \tilde{\mathbf{b}}_\omega(t_0))$.

The matrices $\mathcal{A}(t,\lambda)$, $\mathcal{B}(t,\lambda)$, and $C(t,\lambda)$, are bounded and the system is well defined [11, pag. 626].

If the parameterized system is λ-UGES, then the system (15) is uniformly exponentially stable in $\mathcal{D}_q$ [13, pag.14-15]. The parameterized system verifies the assumptions of [13]:

1) As $\bar{\boldsymbol{\omega}}$ is bounded, the elements of $\mathcal{B}(t,\lambda)$, and

$$\frac{\partial\mathcal{B}(t,\lambda)}{\partial t} = \left[-\frac{1}{2}(\dot{\bar{\mathcal{R}}}^T\mathbf{Q}^T(\tilde{\mathbf{q}}(t,\lambda)) + \bar{\mathcal{R}}^T\mathbf{Q}^T(\dot{\tilde{\mathbf{q}}}(t,\lambda)))\right],$$

are bounded, so there is b_M, such as,

$$\max_{\lambda\in\mathbb{R}_0^+\times\mathcal{D}_q, t\geq0}\left\{\|\mathcal{B}(t,\lambda)\|, \left\|\frac{\partial\mathcal{B}(t,\lambda)}{\partial t}\right\|\right\} \leq b_M,$$

where $\|.\|$ is the induced Euclidean norm of matrices.

2) The matrices

$$P(t,\lambda) = 8K_{b_\omega}\mathbf{I}, \ \ Q(t,\lambda) = 32K_{b_\omega}\tilde{q}_s^2(t,\lambda)K_\omega\mathbf{I},$$

are positive definite, and satisfy

$$\begin{aligned} P(t,\lambda)\mathcal{B}^T(t,\lambda) &= C^T(t,\lambda) \\ -Q(t,\lambda) &= \mathcal{A}^T(t,\lambda)P(t,\lambda) + P(t,\lambda)\mathcal{A}(t,\lambda) + \dot{P}(t,\lambda) \end{aligned}$$

and also satisfy the symmetry conditions, and the existence of q_m, q_M , p_m and p_M, such as,

$$\begin{aligned} q_m\mathbf{I} \leq Q(t,\lambda) \leq q_M\mathbf{I}, \\ p_m\mathbf{I} \leq P(t,\lambda) \leq p_M\mathbf{I}, \end{aligned}$$

with $q_m = 32K_\omega K_{b_\omega}\cos^2\left(\frac{\theta_{max}}{2}\right)$, $q_M = 32K_\omega K_{b_\omega}$, $p_m = p_M = 8K_{b_\omega}$.

The system (16) is λ-UGES if and only if $\mathcal{B}(t,\lambda)$ is λ-uniformly persistently exciting [13]. In order to guarantee that, the sufficient condition $\mathcal{B}(\tau,\lambda)\mathcal{B}^T(\tau,\lambda) \geq \alpha_B\mathbf{I}$ is shown for $\alpha_B > 0$ independently of τ and λ.

$$\begin{aligned} \mathcal{B}(\tau,\lambda)\mathcal{B}^T(\tau,\lambda) &= \left(-\frac{1}{2}\bar{\mathcal{R}}^T\mathbf{Q}^T(\tilde{\mathbf{q}})\right)\left(-\frac{1}{2}\bar{\mathcal{R}}^T\mathbf{Q}^T(\tilde{\mathbf{q}})\right)^T \\ &= \frac{1}{4}\bar{\mathcal{R}}^T\mathbf{Q}^T(\tilde{\mathbf{q}})\mathbf{Q}(\tilde{\mathbf{q}})\bar{\mathcal{R}} \\ &\downarrow \\ \frac{1}{4}\mathbf{y}^T\bar{\mathcal{R}}^T\mathbf{Q}^T(\tilde{\mathbf{q}})\mathbf{Q}(\tilde{\mathbf{q}})\bar{\mathcal{R}}\mathbf{y} &= \frac{1}{4}(\|\mathbf{y}\|^2 - (\mathbf{y}^T\bar{\mathcal{R}}\tilde{\mathbf{q}}_q)^2) \\ &\geq \frac{\|\mathbf{y}\|^2}{4}(1-\|\tilde{\mathbf{q}}_q\|^2) \\ &\geq \frac{\|\mathbf{y}\|^2}{4}\left(1-\sin^2\left(\frac{1}{2}\theta_{max}\right)\right) \\ &\geq \frac{\|\mathbf{y}\|^2}{4}\cos^2\left(\frac{1}{2}\theta_{max}\right) \\ &= \|\mathbf{y}\|^2 c_\theta, \end{aligned}$$

where $c_\theta := \frac{1}{4}\cos^2\left(\frac{1}{2}\theta_{max}\right)$. Then $\mathcal{B}(\tau,\lambda)\mathcal{B}^T(\tau,\lambda) \geq c_\theta\mathbf{I}$ and persistency of excitation condition is satisfied. Consequently, the parameterized system (16) is λ-UGES, and the nonlinear system (15) is exponentially stable in the domain $\mathcal{D}_q$. ■

B. Position Observer

This section derives the position observer based on the IMU acceleration measurements, position readings obtained from range data, and on the attitude observer estimates. The dynamics of the position and velocity estimates are described by

$$\dot{\hat{\mathbf{p}}} = \hat{\mathbf{v}} - (\boldsymbol{\omega}^*)^\wedge \hat{\mathbf{p}} + \mathbf{s}_p,$$
$$\dot{\hat{\mathbf{v}}} = \bar{\mathbf{a}} + \hat{\mathcal{R}}^T {}^L\bar{\mathbf{g}} - (\boldsymbol{\omega}^*)^\wedge \hat{\mathbf{v}} + \mathbf{s}_v,$$

where $\mathbf{s}_p$ and $\mathbf{s}_v$ are the feedback terms that compensate for the estimation errors, and $\boldsymbol{\omega}^*$ is an estimate of the angular velocity obtained from the attitude observer.

Defining the position and velocity errors as $\tilde{\mathbf{p}} := \hat{\mathbf{p}} - \bar{\mathbf{p}}$ and $\tilde{\mathbf{v}} := \hat{\mathbf{v}} - \bar{\mathbf{v}}$, respectively, their dynamics are given by

$$\dot{\tilde{\mathbf{p}}} = \tilde{\mathbf{v}} - (\boldsymbol{\omega}^*)^\wedge \tilde{\mathbf{p}} - (\tilde{\boldsymbol{\omega}})^\wedge \bar{\mathbf{p}} + \mathbf{s}_p, \tag{17}$$
$$\dot{\tilde{\mathbf{v}}} = \left(\hat{\mathcal{R}} - \bar{\mathcal{R}}\right)^T {}^L\bar{\mathbf{g}} - (\boldsymbol{\omega}^*)^\wedge \tilde{\mathbf{v}} - (\tilde{\boldsymbol{\omega}})^\wedge \bar{\mathbf{v}} + \mathbf{s}_v, \tag{18}$$

where $\tilde{\boldsymbol{\omega}} := \boldsymbol{\omega}^* - \bar{\boldsymbol{\omega}}$.

1) Unbiased Angular Velocity Measurement: Assuming that unbiased angular velocity, $\bar{\boldsymbol{\omega}}$ is available and $\boldsymbol{\omega}^* := \bar{\boldsymbol{\omega}}$. The feedback laws are obtain by setting $\mathbf{s}_p$ and $\mathbf{s}_v$ as

$$\mathbf{s}_p = -K_p\left(\hat{\mathbf{p}} - \hat{\mathcal{R}}^T {}^L\bar{\mathbf{p}}\right) \tag{19}$$
$$\mathbf{s}_v = -K_v\left(\hat{\mathbf{p}} - \hat{\mathcal{R}}^T {}^L\bar{\mathbf{p}}\right), \tag{20}$$

where ${}^L\bar{\mathbf{p}}$ is the position of the origin of {B}, relatively to {L}, expressed in {L}.

The dynamics of the position and velocity errors are obtained by replacing (19) and (20), into the errors derivatives (17) and (18), respectively, and can be written as

$$\dot{\tilde{\mathbf{p}}} = \tilde{\mathbf{v}} - (\bar{\boldsymbol{\omega}})^\wedge \tilde{\mathbf{p}} - K_p\left(\hat{\mathbf{p}} - \hat{\mathcal{R}}^T {}^L\bar{\mathbf{p}}\right) \tag{21}$$
$$\dot{\tilde{\mathbf{v}}} = \left(\hat{\mathcal{R}} - \bar{\mathcal{R}}\right)^T {}^L\bar{\mathbf{g}} - (\bar{\boldsymbol{\omega}})^\wedge \tilde{\mathbf{v}} - K_v\left(\hat{\mathbf{p}} - \hat{\mathcal{R}}^T {}^L\bar{\mathbf{p}}\right). \tag{22}$$

By applying a convenient Lyapunov transformation it can be shown that the position observer is globally exponential stable. This is formally stated in Theorem 3.

Assumption 2. *For any $\gamma_p > 0$, there is $k_p > 0$, such that the vehicle position satisfy*

$$\|\bar{\mathbf{p}}(t)\| \;\leq\; k_p e^{\gamma_p (t - t_0)}.$$

Notice that in practice, this assumption is not restrictive, due to the fact that it is trivially verified by physical constraints, not only by the actuators saturation, but also by the intrinsic limitation imposed by the speed of light.

Theorem 3. *Consider $\bar{\mathbf{b}}_\omega = 0$. Let the vehicle position $\bar{\mathbf{p}}$ satisfy Assumption 2 and the conditions of Theorem 1 be verified. Then the estimation errors converge exponentially fast to the equilibrium point $(\tilde{\mathcal{R}}, \tilde{\mathbf{b}}_\omega, \tilde{\mathbf{p}}, \tilde{\mathbf{v}}) = (\mathbf{I}, \mathbf{0}, \mathbf{0})$ for any $(\tilde{\mathbf{p}}, \tilde{\mathbf{v}}) \in \mathbb{R}^3 \times \mathbb{R}^3$. Also, if $\bar{\mathcal{R}}$ and $\bar{\mathbf{b}}_\omega$ are known, the origin of (21, 22) is globally exponentially stable.*

Proof: Since $\tilde{\mathcal{R}} = \hat{\mathcal{R}}\bar{\mathcal{R}}^T$ and $\tilde{\mathbf{p}} = \hat{\mathbf{p}} - \bar{\mathbf{p}}$, then

$$\begin{aligned}\hat{\mathbf{p}} - \hat{\mathcal{R}}^T {}^L\bar{\mathbf{p}} &= \tilde{\mathbf{p}} + \bar{\mathcal{R}}^T {}^L\bar{\mathbf{p}} - \hat{\mathcal{R}}^T {}^L\bar{\mathbf{p}} \\ &= \tilde{\mathbf{p}} + \left(\bar{\mathcal{R}}^T - \bar{\mathcal{R}}^T\tilde{\mathcal{R}}^T\right) {}^L\bar{\mathbf{p}} \\ &= \tilde{\mathbf{p}} + \bar{\mathcal{R}}^T\left(\mathbf{I} - \tilde{\mathcal{R}}^T\right)\bar{\mathcal{R}}\bar{\mathbf{p}}.\end{aligned}$$

Consider the Lyapunov transformation $\bar{\mathcal{R}}$ applied to vectors $\tilde{\mathbf{p}}$ and $\tilde{\mathbf{v}}$. Notice that $\bar{\mathcal{R}}$ is a Lyapunov transformation as it is nonsigular, $\bar{\mathcal{R}}$ and $\dot{\bar{\mathcal{R}}}$ are continuous, and $\bar{\mathcal{R}}$ and $\bar{\mathcal{R}}^{-1}$ are limited. The dynamics of the transformed system are given by

$$\frac{d}{dt}(\bar{\mathcal{R}}\tilde{\mathbf{p}}) = \bar{\mathcal{R}}\tilde{\mathbf{v}} - K_p\bar{\mathcal{R}}\tilde{\mathbf{p}} - K_p\left(\mathbf{I} - \tilde{\mathcal{R}}\right)\bar{\mathcal{R}}\bar{\mathbf{p}} \tag{23}$$
$$\frac{d}{dt}(\bar{\mathcal{R}}\tilde{\mathbf{v}}) = \left(\tilde{\mathcal{R}}^T - \mathbf{I}\right) {}^L\bar{\mathbf{g}} - K_v\tilde{\mathbf{p}} - K_v\left(\mathbf{I} - \tilde{\mathcal{R}}\right)\bar{\mathcal{R}}\bar{\mathbf{p}}, \tag{24}$$

that can be rewritten in condensed form as

$$\dot{\boldsymbol{\xi}} = A\boldsymbol{\xi} + \mathbf{u}, \tag{25}$$

where $\boldsymbol{\xi} = \begin{bmatrix}\bar{\mathcal{R}} & \mathbf{0}_{3\times3} \\ \mathbf{0}_{3\times3} & \bar{\mathcal{R}}\end{bmatrix}\mathbf{x}$, with $\mathbf{x} = [\tilde{\mathbf{p}}\ \tilde{\mathbf{v}}]^T$, $A = \begin{bmatrix}-K_p\mathbf{I}_{3\times3} & \mathbf{I}_{3\times3} \\ -K_v\mathbf{I}_{3\times3} & \mathbf{0}_{3\times3}\end{bmatrix}$, and $\mathbf{u} = \begin{bmatrix}-K_p(\mathbf{I}-\tilde{\mathcal{R}})\bar{\mathcal{R}}\bar{\mathbf{p}} \\ -K_v(\mathbf{I}-\tilde{\mathcal{R}})\bar{\mathcal{R}}\bar{\mathbf{p}} + (\tilde{\mathcal{R}}^T - \mathbf{I})^T {}^L\bar{\mathbf{g}}\end{bmatrix}$. The system (25) is linear time invariant and for $K_p > 0$ and $K_v > 0$, A is Hurwitz, therefore the system is stable.

The input vector $\|\mathbf{u}\|$ verifies

$$\begin{aligned}\|\mathbf{u}\| &\leq K_p\left\|\left(\mathbf{I} - \tilde{\mathcal{R}}\right)\bar{\mathcal{R}}\bar{\mathbf{p}}\right\| + K_v\left\|\left(\mathbf{I} - \tilde{\mathcal{R}}\right)\bar{\mathcal{R}}\bar{\mathbf{p}}\right\| + \left\|\left(\hat{\mathcal{R}} - \bar{\mathcal{R}}\right)^T {}^L\bar{\mathbf{g}}\right\| \\ &\leq \left\|\tilde{\mathcal{R}} - \mathbf{I}\right\|\left((K_p + K_v)\|\bar{\mathbf{p}}\| + \|{}^L\bar{\mathbf{g}}\|\right).\end{aligned}$$

From Theorem 1 and using Assumption 2, it is possible to write

$$\|\mathbf{u}(t)\| \leq k_u e^{-\gamma_u (t - t_0)},$$

where $k_u = 2\left\|\tilde{\mathcal{R}}(t_0) - \mathbf{I}\right\| \max\left\{(K_p + K_v)k_p, \|{}^L\bar{\mathbf{g}}\|\right\}$ and $\gamma_u = \gamma_{\mathcal{R}} - \gamma_p$.

The transformed state $\boldsymbol{\xi}(t)$ satisfies

$$\|\boldsymbol{\xi}(t)\| = e^{A(t-t_0)}\|\boldsymbol{\xi}(t_0)\| + \int_{t_0}^{t} e^{A(t-\tau)}\mathbf{u}(\tau)d\tau.$$

The stability of the origin implies that there exists $k_a, \gamma_a > 0$ such that $\|e^{At}\| \leq k_a e^{-\gamma_a t}$ [11]. And the application of this inequality yields

$$\begin{aligned}\|\boldsymbol{\xi}(t)\| &\leq k_a e^{-\gamma_a (t-t_0)}\|\boldsymbol{\xi}(t_0)\| + k_a k_u \int_{t_0}^{t} e^{-\gamma_a (t-\tau) - \gamma_u (\tau - t_0)} d\tau \\ &= k_a e^{-\gamma_a (t-t_0)}\|\boldsymbol{\xi}(t_0)\| + k_a k_u \frac{e^{-\gamma_u (t-t_0)} - e^{-\gamma_a (t-t_0)}}{\gamma_a - \gamma_u} \\ &\leq k_a e^{-\gamma_a (t-t_0)}\|\boldsymbol{\xi}(t_0)\| + \frac{k_a k_u}{|\gamma_a - \gamma_u|} e^{-\min\{\gamma_u, \gamma_a\}(t-t_0)} \\ &\leq 2\max\left\{k_a\|\boldsymbol{\xi}(t_0)\|, \frac{k_a k_u}{|\gamma_a - \gamma_u|}\right\} e^{-\min\{\gamma_u, \gamma_a\}(t-t_0)}.\end{aligned}$$

Concatenating the attitude and the transformed position estimation errors as $\mathbf{x}_f := \left(\tilde{\mathcal{R}} - \mathbf{I}, \boldsymbol{\xi}\right)$ and using the inequalities $\|\mathbf{x}_f\| \leq \|\tilde{\mathcal{R}} - \mathbf{I}\| + \|\boldsymbol{\xi}\|$ and $\|\tilde{\mathcal{R}} - \mathbf{I}\| \leq \|\mathbf{x}_f\|$, $\|\boldsymbol{\xi}\| \leq \|\mathbf{x}_f\|$, results in the exponential bounds

$$\|\mathbf{x}_f(t)\| \leq k_{\max}\|\mathbf{x}(t_0)\| e^{-\gamma_{\min}(t-t_0)},$$

where $k_{\max} = 2\max\left\{k_{\mathcal{R}}, 2k_a, \frac{4k_a k_{\mathcal{R}}}{|\gamma_a - \gamma_u|}\max\left\{(K_p + K_v)k_p, \|{}^L\bar{\mathbf{g}}\|\right\}\right\}$ and $\gamma_{\min} = \min\left\{\gamma_a, \gamma_{\mathcal{R}} - \gamma_p\right\}$. Hence, the trajectories of the system (7, 25) converge exponentially fast to $(\mathbf{I}, \mathbf{0})$. The fact that $\|\boldsymbol{\xi}(t)\| = \|\mathbf{x}(t)\|$ bears the exponential convergence of cascaded observer (7,21, 22).

If, $\bar{\mathcal{R}}$ is known, then $\mathbf{u}(t) = \mathbf{0}$ and the origin of (25) is globally exponentially stable by the properties of linear time-invariant systems. ■

2) Biased Angular Velocity Measurement: In this section it is assumed that the angular velocity measurements are corrupted by bias and it is required to use an estimate of $\bar{\boldsymbol{\omega}}$, defined as

$$\boldsymbol{\omega}^* := \boldsymbol{\omega}_{sensor} - \hat{\mathbf{b}}_\omega = \bar{\boldsymbol{\omega}} - \tilde{\mathbf{b}}_\omega. \tag{26}$$

The feedback laws are those defined in (19) and (20). Using equations (17), (18), (19), (20) and the definition (26), the position and velocity error dynamics are given by

$$\dot{\tilde{\mathbf{p}}} = \tilde{\mathbf{v}} - (\boldsymbol{\omega}^*)^\wedge \tilde{\mathbf{p}} + (\tilde{\mathbf{b}}_\omega)^\wedge \bar{\mathbf{p}} - K_p \left(\hat{\mathbf{p}} - \hat{\mathcal{R}}^T {}^L\bar{\mathbf{p}}\right) \tag{27}$$

$$\dot{\tilde{\mathbf{v}}} = \left(\hat{\mathcal{R}} - \bar{\mathcal{R}}\right)^T {}^L\bar{\mathbf{g}} - (\boldsymbol{\omega}^*)^\wedge \tilde{\mathbf{v}} + (\tilde{\mathbf{b}}_\omega)^\wedge \bar{\mathbf{v}} - K_v \left(\hat{\mathbf{p}} - \hat{\mathcal{R}}^T {}^L\bar{\mathbf{p}}\right). \tag{28}$$

The statement of Theorem 4, guarantees the exponential convergence of position and velocity estimation errors.

Assumption 3. *For any $\gamma_v > 0$, there exist $k_v > 0$, such that vehicle position and velocity satisfy*

$$\|\mathbf{v}(t)\| \;\leq\; k_v e^{\gamma_v (t-t_0)}.$$

As in Assumption 2, and due to similar reasons, this assumption is not restrictive.

Theorem 4. *Consider the presence of bias in angular velocity measurements. Let Assumption 3 and the conditions of Theorem 2 be satisfied. Then the estimation errors converge exponentially fast to the equilibrium point $(\tilde{\mathcal{R}}, \tilde{\mathbf{b}}_\omega, \tilde{\mathbf{p}}, \tilde{\mathbf{v}}) = (\mathbf{I}, \mathbf{0}, \mathbf{0}, \mathbf{0})$ for any initial condition satisfying* (14) *and $(\tilde{\mathbf{p}}, \tilde{\mathbf{v}}) \in \mathbb{R}^3 \times \mathbb{R}^3$. Also, if $\bar{\mathcal{R}}$ and $\bar{\mathbf{b}}_\omega$ are known, the origin of (27, 28) is globally exponentially stable.*

Proof: Notice that $\hat{\mathbf{p}} - \hat{\mathcal{R}}^T {}^L\bar{\mathbf{p}} = \tilde{\mathbf{p}} + \bar{\mathcal{R}}^T \left(\mathbf{I} - \tilde{\mathcal{R}}^T\right) \bar{\mathcal{R}} \bar{\mathbf{p}}$, and consider the Lyapunov transformation $\mathcal{R}^*$ applied to vectors $\tilde{\mathbf{p}}$, and $\tilde{\mathbf{v}}$, where $\mathcal{R}^* = \mathcal{R}^* (\boldsymbol{\omega}^*)^\wedge$. The dynamics of the transformed system are given by

$$\frac{d}{dt}(\mathcal{R}^* \tilde{\mathbf{p}}) = \mathcal{R}^* \tilde{\mathbf{v}} - K_p \mathcal{R}^* \tilde{\mathbf{p}} + \mathcal{R}^* \tilde{\mathbf{b}}_\omega \bar{\mathbf{p}} - K_p \mathcal{R}^* \bar{\mathcal{R}}^T \left(\mathbf{I} - \tilde{\mathcal{R}}\right) \bar{\mathcal{R}} \bar{\mathbf{p}}$$

$$\frac{d}{dt}(\mathcal{R}^* \tilde{\mathbf{v}}) = \mathcal{R}^* \left(\tilde{\mathcal{R}}^T - \mathbf{I}\right) {}^L\bar{\mathbf{g}} - K_v \mathcal{R}^* \tilde{\mathbf{p}} + \mathcal{R}^* \tilde{\mathbf{b}}_\omega \bar{\mathbf{v}} - K_v \mathcal{R}^* \bar{\mathcal{R}}^T \left(\mathbf{I} - \tilde{\mathcal{R}}\right) \bar{\mathcal{R}} \bar{\mathbf{p}},$$

which can be rewritten in matrix form as

$$\dot{\boldsymbol{\xi}} = A\boldsymbol{\xi} + \mathbf{u} \tag{29}$$

where $\boldsymbol{\xi} = \begin{bmatrix} \mathcal{R}^* & \mathbf{0} \\ \mathbf{0} & \mathcal{R}^* \end{bmatrix} \mathbf{x}$, with $\mathbf{x} = \begin{bmatrix} \tilde{\mathbf{p}}^T & \tilde{\mathbf{v}}^T \end{bmatrix}^T$, $A = \begin{bmatrix} -K_p \mathbf{I} & \mathbf{I} \\ -K_v \mathbf{I} & \mathbf{0} \end{bmatrix}$, and $\mathbf{u} = \begin{bmatrix} \mathcal{R}^* \tilde{\mathbf{b}}_\omega \bar{\mathbf{p}} - K_p \mathcal{R}^* \bar{\mathcal{R}}^T (\mathbf{I} - \tilde{\mathcal{R}}) \bar{\mathcal{R}} \bar{\mathbf{p}} \\ \mathcal{R}^* \tilde{\mathbf{b}}_\omega \bar{\mathbf{v}} - K_v \mathcal{R}^* \bar{\mathcal{R}}^T (\mathbf{I} - \tilde{\mathcal{R}}) \bar{\mathcal{R}} \bar{\mathbf{p}} + \mathcal{R}^* \left(\hat{\mathcal{R}} - \bar{\mathcal{R}}\right)^T {}^L\bar{\mathbf{g}} \end{bmatrix}$. The system (29) is linear time invariant and for $K_p > 0$ and $K_v > 0$ the matrix A is Hurwitz, therefore the system is stable.

From Theorem 2 is known that for K_{b_ω} large enough, there are $k_{\mathcal{R}}, k_b, \gamma_{\mathcal{R}}, \gamma_b > 0$ such that

$$\left\|\tilde{\mathcal{R}}(t) - \mathbf{I}\right\| \leq k_{\mathcal{R}} \left\|\tilde{\mathcal{R}}(t_0) - \mathbf{I}\right\| e^{-\gamma_{\mathcal{R}}(t-t_0)}$$
$$\left\|\tilde{\mathbf{b}}_\omega(t)\right\| \leq k_b \left\|\tilde{\mathbf{b}}_\omega(t_0)\right\| e^{-\gamma_b (t-t_0)}.$$

The input vector $\|\mathbf{u}\|$ verifies the following inequality

$$\|\mathbf{u}\| \leq \|\tilde{\mathbf{b}}_\omega\| \left(\|\bar{\mathbf{p}}\| + \|\bar{\mathbf{v}}\|\right) + \left\|\tilde{\mathcal{R}} - \mathbf{I}\right\| \left((K_p + K_v)\|\bar{\mathbf{p}}\| + \|{}^L\bar{\mathbf{g}}\|\right).$$

Using the fact that $\|\bar{\mathbf{p}}(t)\|$ and $\|\bar{\mathbf{v}}(t)\|$ satisfy respectively Assumption 2 and Assumption 3, it can be shown that

$$\|\mathbf{u}(t)\| \leq k_u e^{-\gamma_u (t-t_0)},$$

where $k_u = 4 \max\left\{k_b \max\left\{k_p, k_v\right\} \|\tilde{\mathbf{b}}_\omega(t_0)\|, k_{\mathcal{R}} \max\left\{(K_p + K_v) k_p, \|{}^L\mathbf{g}\|\right\} \|\tilde{\mathcal{R}}(t_0) - \mathbf{I}\|\right\}$ and $\gamma_u = \min\left\{\gamma_b - \max\left\{\gamma_p, \gamma_v\right\}, \gamma_{\mathcal{R}} - \gamma_p\right\}$, that is positive since γ_p and γ_v can be made as small as desired by Assumption 2 and Assumption 3. The transformed state $\boldsymbol{\xi}(t)$ satisfies

$$\|\boldsymbol{\xi}(t)\| = e^{A(t-t_0)} \|\boldsymbol{\xi}(t_0)\| + \int_{t_0}^{t} e^{A(t-\tau)} \mathbf{u}(\tau) d\tau,$$

and by [11] the stability of the origin implies that there exists $k_a, \gamma_a > 0$ such that $\|e^{At}\| \leq k_a e^{-\gamma_a t}$, therefore the subsequent inequality holds

$$\begin{aligned}
\|\boldsymbol{\xi}(t)\| &\leq k_a e^{-\gamma_a (t-t_0)} \|\boldsymbol{\xi}(t_0)\| + k_a k_u \int_{t_0}^{t} e^{-\gamma_a (t-\tau) - \gamma_u (\tau - t_0)} d\tau \\
&= k_a e^{-\gamma_a (t-t_0)} \|\boldsymbol{\xi}(t_0)\| + k_a k_u \frac{e^{-\gamma_u (t-t_0)} - e^{-\gamma_a (t-t_0)}}{\gamma_a - \gamma_u} \\
&\leq k_a e^{-\gamma_a (t-t_0)} \|\boldsymbol{\xi}(t_0)\| + \frac{k_a k_u}{|\gamma_a - \gamma_u|} e^{-\min\{\gamma_u, \gamma_a\}(t-t_0)} \\
&\leq 2 \max\left\{k_a \|\boldsymbol{\xi}(t_0)\|, \frac{k_a k_u}{|\gamma_a - \gamma_u|}\right\} e^{-\min\{\gamma_u, \gamma_a\}(t-t_0)}.
\end{aligned}$$

Concatenating the attitude and transformed position estimation errors as $\mathbf{x}_f := \left(\tilde{\mathcal{R}} - \mathbf{I}, \tilde{\mathbf{b}}_\omega, \boldsymbol{\xi}\right)$ and using the inequalities $\|\mathbf{x}_f\| \leq \|\tilde{\mathcal{R}} - \mathbf{I}\| + \|\tilde{\mathbf{b}}_\omega\| + \|\boldsymbol{\xi}\|$ and $\max\{\|\tilde{\mathcal{R}} - \mathbf{I}\|, \|\tilde{\mathbf{b}}_\omega\|, \|\boldsymbol{\xi}\|\} \leq \|\mathbf{x}_f\|$, an exponential upper bound is given by

$$\|\mathbf{x}_f(t)\| \leq k_{\max} \|\mathbf{x}_f(t_0)\| e^{-\gamma_{\min}(t-t_0)},$$

where $k_{\max} = 3 \max\left\{k_{\mathcal{R}}, k_b, 2k_a, \frac{8 k_a k_b \max\{k_p, k_v\}}{|\gamma_a - \gamma_u|}, \frac{8 k_a k_{\mathcal{R}} \max\{(K_p, K_v) k_p, \|{}^L\mathbf{g}\|\}}{|\gamma_a - \gamma_u|}\right\}$, and $\gamma_{\min} = \min\left\{\gamma_a, \gamma_b - \max\left\{\gamma_p, \gamma_v\right\}, \gamma_{\mathcal{R}} - \gamma_p\right\}$.

Hence, the trajectories of the system (13,29) converge exponentially fast to the origin. The fact that $\|\boldsymbol{\xi}(t)\| = \|\mathbf{x}(t)\|$ bears the exponential convergence of cascaded observer (13, 27, 28).

If $\bar{\mathcal{R}}$ and $\bar{\mathbf{b}}_\omega$ are known, then $\mathbf{u}(t) = \mathbf{0}$ and the origin of (29) is globally exponentially stable by the properties of linear time-invariant systems. ■

C. Feedback Terms as Explicit Functions of Sensors Readings

One important advantage of the derived observers, is that the feedback terms can be written as explicit functions of the sensor readings. For both position observers the feedback terms are given by

$$\mathbf{s}_p = -K_p \left(\hat{\mathbf{p}} - \hat{\mathcal{R}}^L \bar{\mathbf{p}}\right)$$
$$\mathbf{s}_v = -K_v \left(\hat{\mathbf{p}} - \hat{\mathcal{R}}^L \bar{\mathbf{p}}\right).$$

For the unbiased angular velocity attitude observer the feedback term is given by

$$\hat{\boldsymbol{\omega}} = \boldsymbol{\omega}_{sensor} - K_\omega \mathbf{s}_\omega,$$

and for the observer that estimates the bias present in angular velocity measurements, can written as

$$\hat{\boldsymbol{\omega}} = \boldsymbol{\omega}_{sensor} - \hat{\mathbf{b}}_\omega - K_\omega \mathbf{s}_\omega.$$

The vector ${}^L\bar{\mathbf{p}}$ is computed directly from range measurements using a spherical interpolation algorithm. The dependence of $\mathbf{s}_\omega$ on the sensor readings, was derived in [26,

Theorem 9]. In the case of rank($\mathbf{X}$) ≥ 3

$$\mathbf{s}_\omega = \sum_{i=1}^{n} \left(\hat{\mathcal{R}}^T \mathbf{X}\mathbf{D}_X\mathbf{A}_X\mathbf{e}_i\right) \times \left(\bar{\mathbf{B}}\mathbf{D}_X\mathbf{A}_X\mathbf{e}_i\right),$$

where $\mathbf{A}_X$ is such that $\mathbf{U}_X\mathbf{U}_X^T = \mathbf{I}$, $\mathbf{U}_X = \bar{\mathcal{R}}\bar{\mathbf{U}}\mathbf{D}_X\mathbf{A}_X$ and $\mathbf{e}_i$ is the unit vector along the *i-th* axis. In the case of rank($\mathbf{X}$) = 2

$$\mathbf{s}_\omega = \sum_{i=1}^{n} \left(\hat{\mathcal{R}}^T \mathbf{H}_a\mathbf{A}_{Xa}\mathbf{e}_i\right) \times \left(\bar{\mathbf{B}}_a\mathbf{A}_{Xa}\mathbf{e}_i\right),$$

where

$$\mathbf{H}_a = \left[\mathbf{X}\mathbf{D}_X \;\; \mathbf{X}\mathbf{D}_X\mathbf{e}_i \times \mathbf{X}\mathbf{D}_X\mathbf{e}_j\right], \; i \neq j$$
$$\bar{\mathbf{B}}_a = \left[\bar{\mathbf{B}}\mathbf{D}_X \;\; \bar{\mathbf{B}}\mathbf{D}_X\mathbf{e}_i \times \bar{\mathbf{B}}\mathbf{D}_X\mathbf{e}_j\right], \; i \neq j,$$

and $\mathbf{A}_{Xa}$ is such that $\mathbf{U}_{Xa}\mathbf{U}_{Xa}^T = \mathbf{I}$, with

$$\mathbf{U}_{Xa} := \mathbf{H}_a\mathbf{A}_{Xa}.$$

IV. NUMERIC INTEGRATION ON SO(3)

Many dynamic systems described by differential equations have some properties that are preserved in time, like energy, linear and angular momentum, and algebraic constraints on the solution. Typically, these restrictions force the solution of the differential equations to evolve in specific manifolds. The classical numerical integration algorithms were designed to work in $\mathbb{R}^n$ and naturally do not preserve some of the desired properties.

A particular case corresponds to the set of all rotation matrices, termed the Special Orthogonal group, and denoted by SO(3). Any matrix $\mathcal{R}$ of this group has the properties

$$\mathcal{R}\mathcal{R}^T = \mathbf{I}_{3\times3} \tag{30}$$
$$\det(\mathcal{R}) = 1, \tag{31}$$

which are not preserved by the classical numerical integration algorithms like Runge-Kutta methods. In fact it can be shown that Runge-Kutta integration techniques do not preserve polynomial invariants, like determinant of degree n, with $n \geq 3$ [8, Theorem IV.3.3]. To overcome this issue there is the possibility of parameterize the rotation matrix.

The two commonest rotation matrix parameterizations are *Euler angles*, and *quaternions*. The first, has three independent parameters but suffers from singularities which is not desirable in applications like the one targeted in the present paper. The second, has no singularities, but requires the use of four parameters and presents an extra constrain on the norm. This forces, when using classical integration algorithms, a quaternion normalization at each integration step.

This section presents three numerical algorithms designed for right-invariant differential equations of the form $\dot{Y} = A(t, Y)Y$, evolving on Lie Groups, namely the *Crouch-Grossman Method* [6], the *Munthe-Kaas Method* [16] and the *Commutator-Free Lie Group Method* [4]. These methods can be applied to differential equations on SO(3) and naturally preserve the properties (30) and (31). An application of these methods to multi-body dynamics evolving in SE(3) can be found in [21]. The accuracy of these techniques is indicated by the order condition, see [8] for further details.

The *Crouch-Grossman Method* (CG), presented in [6] is described by the following generic algorithm

$$\begin{aligned} Y^{(i)} &= \mathrm{Exp}(Ta_{i,i-1}K^{(i-1)}) \ldots \mathrm{Exp}(Ta_{i,1}K^{(1)})Y_{k-1} \\ K^{(i)} &= A\left(t_{k-1} + Tc_i, Y^{(i)}\right) \\ Y_k &= \mathrm{Exp}(Tb_sK^{(s)}) \ldots \mathrm{Exp}(Tb_1K^{(1)})Y_{k-1}. \end{aligned} \tag{32}$$

where T is the integration period, and Exp(.) the exponential map in SO(3) that can efficiently computed using the so-called Rodrigues Formula

$$\mathrm{Exp}((\boldsymbol{\omega})^\wedge) = \begin{cases} \mathbf{I}, & \text{if } \|\boldsymbol{\omega}\| = 0, \\ \mathbf{I} + \frac{\sin(\|\boldsymbol{\omega}\|)}{\|\boldsymbol{\omega}\|}(\boldsymbol{\omega})^\wedge + \frac{\sin^2\left(\frac{\|\boldsymbol{\omega}\|}{2}\right)}{\frac{\|\boldsymbol{\omega}\|^2}{2}}\left((\boldsymbol{\omega})^\wedge\right)^2, & \text{if } \|\boldsymbol{\omega}\| \neq 0. \end{cases} \tag{33}$$

The interested reader can find the coefficients, $a_{(.)}$, $b_{(.)}$, and $c_{(.)}$, for CG method, up to the sixth order in [9, 20, 10].

With *Munthe-Kaas Method* (MK) [16], coefficients for standard Runge-Kutta methods can be used. This method is implemented by the following algorithm

$$\begin{aligned} \Theta^{(i)} &= T\sum_{j=1}^{i-1} a_{ij}F^{(j)} \\ Y^{(i)} &= \mathrm{Exp}\left(\Theta^{(i)}\right)Y_{k-1} \\ F^{(i)} &= \mathrm{Dexp}^{-1}\left(\Theta^{(i)}\right)A\left(t_{k-1} + Tc_i, Y^{(i)}\right) \\ \Theta &= T\sum_{i=1}^{s} b_iF^{(i)} \\ Y_k &= \mathrm{Exp}(\Theta)Y_{k-1}, \end{aligned} \tag{34}$$

where $\mathrm{Dexp}^{-1}(.)$ is the inverse of the differential of the exponential map, which in SO(3) can be computed through the explicit formula [21]

$$\mathrm{Dexp}^{-1}((\boldsymbol{\omega})^\wedge) = \begin{cases} \mathbf{I}, & \text{if } \|\boldsymbol{\omega}\| = 0, \\ \mathbf{I} - \frac{1}{2}(\boldsymbol{\omega})^\wedge - \frac{\|\boldsymbol{\omega}\|\cot\left(\frac{\|\boldsymbol{\omega}\|}{2}\right)-2}{2\|\boldsymbol{\omega}\|^2}\left((\boldsymbol{\omega})^\wedge\right)^2, & \text{if } \|\boldsymbol{\omega}\| \neq 0. \end{cases} \tag{35}$$

Finally the *Commutator-Free Lie Group Method* (CF), presented in [4], is given by the algorithm

$$\begin{aligned} Y^{(i)} &= \mathrm{Exp}\left(\sum_j^s Ta_{ij}^{[k]}K^{(j)}\right) \ldots \mathrm{Exp}\left(\sum_j^s Ta_{ij}^{[1]}K^{(j)}\right)Y_{k-1} \\ K^{(i)} &= A\left(t_{k-1} + Tc_i, U^{(i)}\right) \\ Y_k &= \mathrm{Exp}\left(\sum_j^s Tb_j^{[k]}K^{(j)}\right) \ldots \mathrm{Exp}\left(\sum_j^s Tb_j^{[1]}K^{(j)}\right)Y_{k-1}. \end{aligned} \tag{36}$$

The coefficients of this method for the third and the fourth orders can be found in [21]. The coefficients for second order were not found in literature.

The application of the third order coefficients from [21, Table II(a)] results in

$$\begin{aligned} Y^{(1)} &= Y_{k-1}, \;\; K^{(1)} = A\left(t_{k-1}, Y^{(1)}\right) \\ Y^{(2)} &= \mathrm{Exp}\left(\frac{T}{3}K^{(1)}\right)Y_{k-1}, \;\; K^{(2)} = A\left(t_{k-1} + \frac{T}{3}, Y^{(2)}\right) \\ Y^{(3)} &= \mathrm{Exp}\left(\frac{2T}{3}K^{(2)}\right)Y_{k-1}, \;\; K^{(3)} = A\left(t_{k-1} + \frac{2T}{3}, Y^{(3)}\right) \\ Y_k &= \mathrm{Exp}\left(-\frac{T}{12}K^{(1)} + \frac{3T}{4}K^{(3)}\right)\mathrm{Exp}\left(\frac{T}{3}K^{(1)}\right)Y_{k-1}. \end{aligned}$$

It is possible to save the computation of some of the exponentials by reusing exponentials previously computed. Therefore, for third order method one can have

$$Y_k = \mathrm{Exp}\left(-\frac{T}{12}K^{(1)} + \frac{3T}{4}K^{(3)}\right)Y^{(2)}$$

saving the computation of one exponential map and one matrix multiplication.

Also in the fourth order case savings are possible. One can implement this method by using the coefficients presented in Table II(b) from [21]:

$$\begin{aligned}
Y^{(1)} &= Y_{k-1},\ K^{(1)} = A\left(t_{k-1}, Y^{(1)}\right)\\
Y^{(2)} &= \mathrm{Exp}\left(\frac{T}{2}K^{(1)}\right)Y_{k-1},\ K^{(2)} = A\left(t_{k-1}+\frac{T}{2}, Y^{(2)}\right)\\
Y^{(3)} &= \mathrm{Exp}\left(\frac{T}{2}K^{(2)}\right)Y_{k-1},\ K^{(3)} = A\left(t_{k-1}+\frac{T}{2}, Y^{(3)}\right)\\
Y^{(4)} &= \mathrm{Exp}\left(-\frac{T}{2}K^{(1)} + K^{(3)}\right)Y^{(2)},\ K^{(4)} = A\left(t_{k-1}+T, Y^{(4)}\right)\\
Y_k &= \mathrm{Exp}\left(-\frac{T}{12}K^{(1)} + \frac{T}{6}K^{(2)} + \frac{T}{6}K^{(3)} + \frac{T}{4}K^{(4)}\right)\\
&\quad \mathrm{Exp}\left(\frac{T}{4}K^{(1)} + \frac{T}{6}K^{(2)} + \frac{T}{6}K^{(3)} - \frac{T}{12}K^{(4)}\right)Y_{k-1}.
\end{aligned}$$

The analysis of complexity of each of these methods up to the fourth order, is presented in Table I.

TABLE I
COMPLEXITY OF EACH STEP OF *CG*, *MK* E *CF*, FOR THE SECOND, THIRD AND FOURTH ORDERS.

operation	Exp[a]	Dexp^{-1}[b]	*mmult*[c]
CG 2nd order	3	0	3
MK 2nd order	2	1	3
CG 3rd order	6	0	6
MK 3rd order	3	2	5
CF 3rd order	3	0	3
CG 4th order	15	0	15
MK 4th order	4	3	7
CF 4th order	5	0	5

[a] exponential map
[b] inverse of differential of exponential map
[c] 3×3 matrix multiplication

V. OBSERVER DISCRETE TIME IMPLEMENTATION

This section presents a discrete time implementation of the pose observer proposed in Section III. This implementation will be obtained by applying the discrete time integration methods discussed in Section IV to the observer continuous time dynamics. The integration method selected to obtain the discrete time implementation should be the most adequate to guarantee that the latter approximates conveniently the original continuous time observer. During the selection procedure one has to take into account the quality of the sensor suite, the desired sampling rate and the computational resources available. In general, higher order methods will lead to better approximations involving a higher computational costs. However, the quality of the results obtained will be always limited by the quality of data sets available from the sensor suite.

A. Numeric Integration of the Attitude Observer

The attitude observer dynamics is composed by two differential equations. One that evolves in SO(3), (2), and another in $\mathbb{R}^3$, (12). The first can be integrated resorting to one of the methods proposed in Section IV, and the second to any classical numeric integration technique.

The equation (2) of observer dynamics it is not in the general form $\dot{Y} = A(t, Y)Y$, although a equivalent equation in the desired form can be obtained by transposing (2) which gives

$$\left(\dot{\hat{\mathcal{R}}}\right)^T = \left(\hat{\mathcal{R}}(\hat{\boldsymbol{\omega}})^\wedge\right)^T \Leftrightarrow \dot{\hat{\mathcal{R}}}^T = -(\hat{\boldsymbol{\omega}})^\wedge\hat{\mathcal{R}}^T.$$

Notice that in the present case $\hat{\boldsymbol{\omega}}$ is independent of $\hat{\mathcal{R}}$ allowing for a substantial simplification of the integration algorithms.

The presented geometric numerical integration algorithms require the knowledge of the function $\hat{\boldsymbol{\omega}}(t)$ in instants between sampling times. Different sampling and computation strategies can be adopted to obtain an approximation of this function using methods such as polynomial interpolation of the sampled data. In the present case, as the target was the implementation using tactical grade inertial sensors and the use of limited computational resources, the selected method was the linear interpolation of $\hat{\boldsymbol{\omega}}$ in the interval $[(k-1)T,\ kT]$ that is

$$\hat{\boldsymbol{\omega}}(t) \approx \left(\frac{\hat{\boldsymbol{\omega}}(kT) - \hat{\boldsymbol{\omega}}(kT-T)}{T}\right)(t - (kT-T)) + \hat{\boldsymbol{\omega}}(kT-T). \qquad (37)$$

The linear interpolation adopted for $\hat{\boldsymbol{\omega}}$ limits the order of the integration technique as the maximal precision is achieved for second order methods and an increase on the order of the method will not impact on the precision of the result. Table II shows the number of operations required in each step of second order CG and MK methods, and third order CF method. From the table it can be concluded that all three integration techniques present similar complexity being the MK a little less computationally expensive. For this reason was selected to implement equation (2).

TABLE II
COMPLEXITY IN EACH STEP FOR CG, MK AND LC METHODS.

operation	Exp	Dexp^{-1}	*mmult*
CG 2nd order	2	0	2
MK 2nd order	1	1	2
CF 3rd order	2	0	2

Finally, the discrete time implementation of equation (12) was obtained by using a second order *Adams-Moulton Method*, see [3] for further details. This selection was done based on similar arguments as those used for (2). The resulting attitude observer numerical integration algorithm can be summarized as

$$\begin{aligned}
\hat{\mathbf{b}}_{\omega\ k} &= \hat{\mathbf{b}}_{\omega\ k-1} + \frac{T}{2}\left(K_{b_\omega}\mathbf{s}_{\omega\ k} + K_{b_\omega}\mathbf{s}_{\omega\ k-1}\right)\\
F^{(1)} &= -\hat{\boldsymbol{\omega}}(kT-T)^\wedge\\
\Theta^{(2)} &= \frac{T}{2}F^{(1)}\\
F^{(2)} &= -\,\mathrm{Dexp}^{-1}\left(\Theta^{(2)}\right)\hat{\boldsymbol{\omega}}\left(kT-\frac{T}{2}\right)^\wedge\\
\hat{\mathcal{R}}_k^T &= \mathrm{Exp}\left(TF^{(2)}\right)\hat{\mathcal{R}}_{k-1}^T.
\end{aligned}$$

Since this is an implicit algorithm a numeric technique like the *Fixed-Point Method* should be run at in each integration step.

B. Numeric Integration of the Position Observer

The numerical integration of the differential equations associated to the position observer, (27) and (28) both in $\mathbb{R}^3$, was performed by resorting to a second order *Adams-Moulton Method*. The resulting numerical integration algorithm is described as follows

$$
\begin{aligned}
g_{p\ k} &= \hat{\mathbf{v}}_k - (\hat{\boldsymbol{\omega}}_k)^{\wedge}\hat{\mathbf{p}}_k - K_p(\hat{\mathbf{p}}_k - \hat{\mathcal{R}}_k^{T\,L}\bar{\mathbf{p}}_k)\\
\hat{\mathbf{p}}_k &= \hat{\mathbf{p}}_{k-1} + \frac{T}{2}\left(g_{p\ k} + g_{p\ k-1}\right)\\
g_{v\ k} &= \bar{\mathbf{a}}_k + \hat{\mathcal{R}}_k^{T\,L}\bar{\mathbf{g}} - (\hat{\boldsymbol{\omega}}_k)^{\wedge}\hat{\mathbf{v}}_k - K_v(\hat{\mathbf{p}}_k - \hat{\mathcal{R}}_k^{T\,L}\bar{\mathbf{p}}_k)\\
\hat{\mathbf{v}}_k &= \hat{\mathbf{v}}_{k-1} + \frac{T}{2}\left(g_{v\ k} + g_{v\ k-1}\right).
\end{aligned}
$$

As this is implicit algorithm it is also required to use a numeric method at each integration step.

VI. SIMULATIONS

In this section, simulation results obtained for the continuous time observer and for its discrete time implementation are presented and discussed. In the simulation the sampling frequency of the observer discrete time implementation was set to 50 Hz. Five beacons were placed in the mission scenario located at ${}^L\bar{\mathbf{x}}_1 = [20\ 20\ 20]^T$ m, ${}^L\bar{\mathbf{x}}_2 = [-20\ -20\ 20]^T$ m, ${}^L\bar{\mathbf{x}}_3 = [20\ -20\ -20]^T$ m, ${}^L\bar{\mathbf{x}}_4 = [-20\ 20\ -20]^T$ m, and ${}^L\bar{\mathbf{x}}_5 = [0\ 0\ 0]^T$ m. The acoustic receivers installed in body frame were placed in ${}^B\mathbf{r}_1 = [0\ 0\ 0]^T$ m, ${}^B\mathbf{r}_2 = [0.5\ 0\ 0]^T$ *m*, ${}^B\mathbf{r}_3 = [0\ 0.5\ 0]^T$ m, and ${}^B\mathbf{r}_4 = [0\ 0\ 0.5]^T$ m. The vehicle trajectory is characterized by oscillatory acceleration and angular velocity with frequency 1/2 Hz.

The feedback gains were set to $K_\omega = 2$, $K_{b_\omega} = 2$, $K_p = 2$, and $K_v = 2$. Notice that The gains K_ω, K_{b_ω}, K_p, and K_v, verify the condition (14), that is $\frac{\frac{1}{K_{b_\omega}}\|\tilde{\mathbf{b}}_\omega(t_0)\|^2}{4(1+\cos(\theta(t_0)))} \approx 0.065 < 1$. The initial errors were assumed as $\tilde{\mathbf{p}}(t_0) = [3\ 3\ 3]^T$ m, $\tilde{\mathbf{v}}(t_0) = [1\ 1\ 1]^T$ ms^{-1}, $\theta(t_0) = 135\frac{\pi}{180}$ rad, and $\mathbf{b}_\omega(t_0) = \frac{\pi}{180}[5\ 5\ 5]^T$ rads^{-1}, the initial bias estimates were set to zero in all three channels.

Figures 3 and 4 illustrate the estimation errors of the continuous time observer and of its discrete time implementation. The quality of the observer' discrete time implementation can be inferred from Figures 5 and 6 where a detail of the differences between the estimates produced by the continuous time observer and those obtained with the discrete time implementation are depicted.

VII. CONCLUSIONS

In this work, a nonlinear attitude and position observer using inertial sensor measurements and ranges to acoustic beacons, was derived. The observers have a cascade topology. The attitude observer was extended to estimate the existence of static bias in angular velocity measurements. It was proved the exponentially fast convergence to the origin of the estimation errors. The feedback laws were shown to be explicit functions of the sensor readings. A method to obtain a discrete time

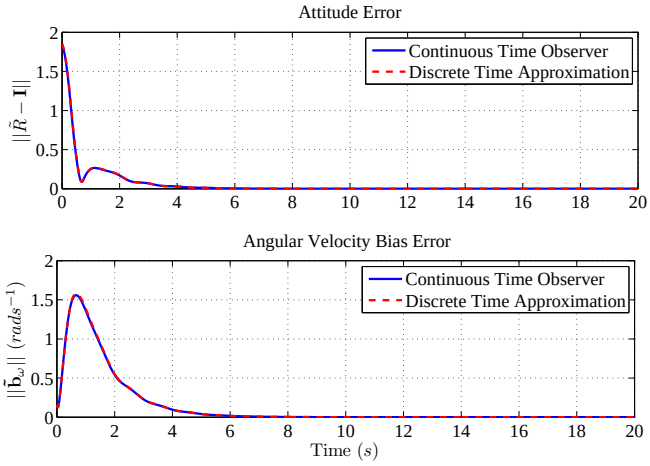

Fig. 3. Attitude and angular velocity bias estimates

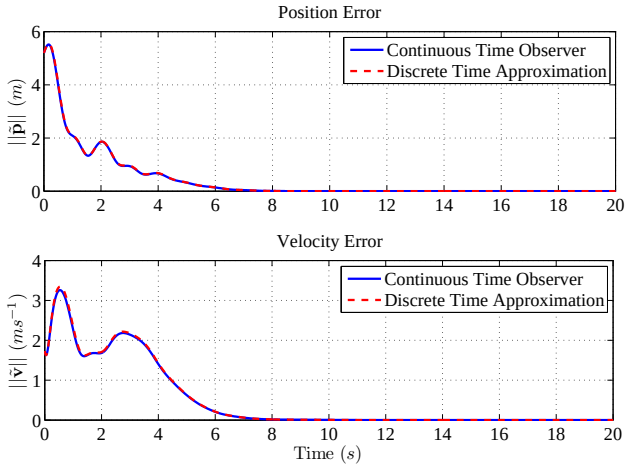

Fig. 4. Position and velocity estimates

implementation of the attitude observer using recent results from numeric integration in Lie groups was proposed, and a discrete implementation of the attitude and position observers was obtained. Simulations results illustrate the convergence to the origin of the estimation errors and the quality of the proposed discrete time implementation.

Future work will focus on the implementation and validation of the proposed algorithm in a real time architecture onboard an Unmanned Aerial Vehicle.

Appendix A
Beacons Positions Augmentation

Assumption 1 establishes that $\text{rank}(\mathbf{X}) \geq 2$ which, given that $\mathbf{H} = \mathbf{X}\mathbf{D}_X$, is equivalent to $\text{rank}(\mathbf{H}) = \text{rank}\left(\begin{bmatrix}\mathbf{H} & 0\end{bmatrix}\right) := \text{rank}\left(\mathbf{X}\begin{bmatrix}\mathbf{D}_X & \mathbf{1}_n\end{bmatrix}\right) = \text{rank}(\mathbf{X}) \geq 2$. However, the coordinate transformation of Proposition 1 requires that $\mathbf{H}$ is full rank. If $\text{rank}(\mathbf{X}) = 2$, it is possible to augment matrix $\mathbf{H}$ to produce $\mathbf{H}_a$ such that $\text{rank}(\mathbf{H}_a) = 3$. Taking two linearly independent columns of $\mathbf{H}$, ${}^L\mathbf{h}_i$ and ${}^L\mathbf{h}_j$, the augmented matrix is given by $\mathbf{H}_a = \begin{bmatrix}\mathbf{H} & {}^L\mathbf{h}_i \times {}^L\mathbf{h}_j\end{bmatrix}$, which is full rank. Defining $\mathbf{U}_{Xa} := \mathbf{H}_a\mathbf{A}_{Xa}$, by the steps of the proof of Proposition 1 there is $\mathbf{A}_{Xa} \in \text{M}(n+1)$ nonsingular such that $\mathbf{U}_{Xa}\mathbf{U}_{Xa}^T = \mathbf{I}$,

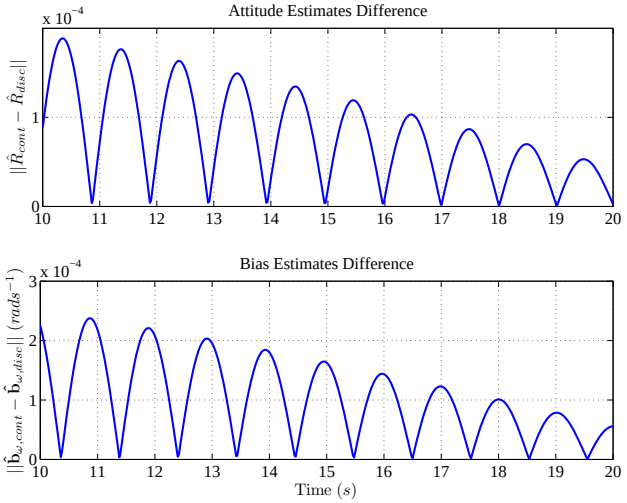

Fig. 5. Difference of attitude and angular velocity bias estimates

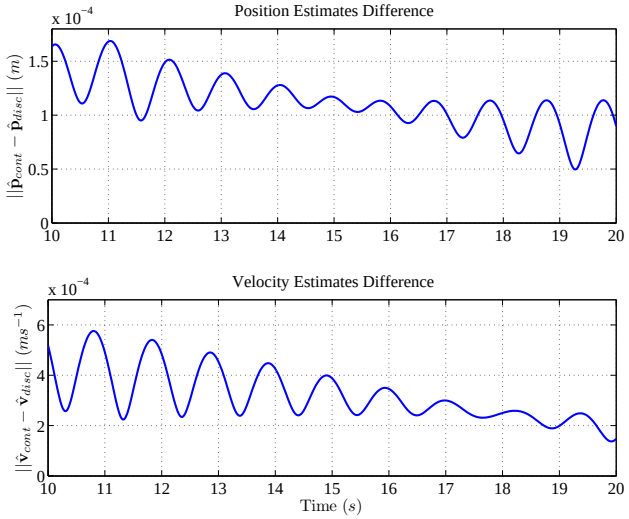

Fig. 6. Difference of position and velocity estimates

as desired. The cross product is commutable with coordinate transformations, $(\mathcal{R}^{T\,L}\mathbf{h}_i) \times (\mathcal{R}^{T\,L}\mathbf{h}_j) = \mathcal{R}^T({}^L\mathbf{h}_i \times {}^L\mathbf{h}_j)$, so the representation of the augmented matrices in body coordinates is simply given by ${}^B\bar{\mathbf{U}}_{Xa} = \bar{\mathcal{R}}^T\mathbf{U}_{Xa}$ and ${}^B\hat{\mathbf{U}}_{Xa} = \hat{\mathcal{R}}^T\mathbf{U}_{Xa}$. The modified observer is obtained by replacing $\mathbf{U}_X$, $\mathbf{H}$ and $\mathbf{A}_X$ by $\mathbf{U}_{Xa}$, $\mathbf{H}_a$ and $\mathbf{A}_{Xa}$.

References

[1] P. Batista, C. Silvestre, and P. Oliveira. Position and velocity navigation filters for marine vehicles. In *17th IFAC World Congress*, South Korea, Seul, Jul. 2008.

[2] S. P. Bhat and D. S. Bernstein. A topological obstruction to continuous global stabilization of rotational motion and the unwinding phenomenon. *Systems and Control Letters*, 39(1):63–70, Jan. 2000.

[3] R.L. Burden and J.D. Faires. *Numerical Analysis*. PWS-KENT Publishing Company, Boston, 1993.

[4] E. Celledoni, A. Marthinsen, and B. Owren. Commutator-free Lie group methods. *Future Generation Computer Systems*, 19(3):341–352, Abr. 2003.

[5] N. Chaturvedi and N. McClamroch. Almost global attitude stabilization of an orbiting satellite including gravity gradient and control saturation effects. In *2006 American Control Conference*, Minnesota, USA, Jun. 2006.

[6] P. E. Crouch and R. Grossman. Numerical integration of ordinary differential equations on manifolds. *J. Nonlinear Science*, 3:1–33, 1993.

[7] D. Fragopoulos and M. Innocenti. Stability considerations in quaternion attitude control using discontinuous Lyapunov functions. *IEEE Proceedings on Control Theory and Applications*, 151(3):253– 258, May 2004.

[8] E. Hairer, C. Lubich, and G. Wanner. *Geometric Numerical Integration: Structure-Preserving Algorithms for Ordinary Differential Equations*. Springer, New York, 2002.

[9] E. Hairer, C. Lubich, and G. Wanner. *Geometric Numerical Integration, Structure-Preserving Algorithms for Ordinary Differential Equations*, volume 31 of *Springer Series in Computational Mathematics*. Springer, second edition, 2006.

[10] Z. Jackiewicz, A. Marthinsen, and B. Owren. Construction of Runge-Kutta Methods of Crouch-Grossman type of high order. *Adv. Computat. Math.*, 13(4):405–415, 2000.

[11] H. K. Khalil. *Nonlinear Systems*. Prentice Hall, second edition, 1996.

[12] D. E. Koditschek. The Application of Total Energy as a Lyapunov Function for Mechanical Control Systems. *Control Theory and Multibody Systems*, 97:131–151, 1989.

[13] A. Loría and E. Panteley. Uniform exponential stability of linear time-varying systems: revisited. *Systems and Control Letters*, 47(1):13–24, Set. 2002.

[14] R. Mahony, T. Hamel, and J. Pflimlin. Non-linear complementary filters on the Special Orthogonal Group. *IEEE Transactions on Automatic Control*, 53(5):1203–1218, Jun. 2008.

[15] M. Malisoff, M. Krichman, and E. Sontag. Global stabilization for systems envolving on manifolds. *Journal of Dynamical and Control Systems*, 12(2):161–184, Apr. 2006.

[16] H. Munthe-Kaas. High order Runge-Kutta methods on manifolds. *Appl. Numer. Math.*, 29(1):115–127, 1999.

[17] H. Z. Munthe-Kaas. Runge-Kutta methods on Lie groups. *BIT*, 38(1):92–11, 1998.

[18] R. M. Murray, Z. Li, and S. S. Sastry. *A Mathematical Introduction to Robotic Manipulation*. CRC, 1994.

[19] B. Owren. Order conditions for commutator-free Lie group methods. *J. Phys. A: Math. Gen.*, 39:5585–5599, 2006.

[20] B. Owren and A. Marthinsen. Runge-Kutta methods adapted to manifolds and based on rigid frames. *BIT Numerical Mathematics*, 39(1):116–142, 1999.

[21] Jonghoon Park and Wan-Kyun Chung. Geometric integration on Euclidean group with application to articulated multibody systems. *IEEE Transactions on Robotics*, 21(5):850–863, Oct. 2005.

[22] S. Salcudean. A globally convergent angular velocity observer for rigid body motion. *IEEE Transactions on Automatic Control*, 36(12):1493–1497, Dec. 1991.

[23] J. O. Smith and J. S. Abel. The spherical interpolation method of source localization. *IEEE Journal of Oceanic Engineering*, 12(1):246–252, Jan. 1987.

[24] J. Thienel and R. M. Sanner. A coupled nonlinear spacecraft attitude controller and observer with an unknown constant gyro bias and gyro noise. *IEEE Transactions on Automatic Control*, 48(11):2011–2015, Nov. 2003.

[25] J. Vasconcelos, R. Cunha, C. Silvestre, and P. Oliveira. Landmark based nonlinear observer for rigid body attitude and position estimation. In *46th IEEE Conference on Decision and Control*, Dec. 2007.

[26] J. Vasconcelos, R. Cunha, C. Silvestre, and P. Oliveira. Landmark based nonlinear observer for rigid body attitude and position estimation. In *17th IFAC World Congress*, South Korea, Seul, Jul. 2008.

[27] J. Vasconcelos, C. Silvestre, and P. Oliveira. A nonlinear GPS/IMU based observer for rigid body attitude and position estimation. In *47th IEEE Conference on Decision and Control*, Cancun, Mexico, Dec. 2008.